Facile assembly of 2D Ni-based coordination polymer nanosheets as battery-type electrodes for high-performance supercapacitors

Qinghai Ma[a], Fang Cui[*a], Mufei Liu[b], Jiajia Zhang[a], Tieyu Cui[*a]

[a.] *School of Chemistry and Chemical Engineering, Harbin Institute of Technology, Harbin, 150001, P.R. China.*

[b.] *College of Chemical Engineering, China University of Petroleum (East China), Qingdao, 266580, P.R. China*

*Corresponding Authors: Fax: (+86) 0451-86403646

E-mail: cuifang@hit.edu.cn (F. Cui)，cuit@hit.edu.cn (T. Y. Cui)

Fig. S1 Image showing the formation of a green precipitate ($Ni(MAA)_2$ nanosheets, named Ni-nCPs-1).

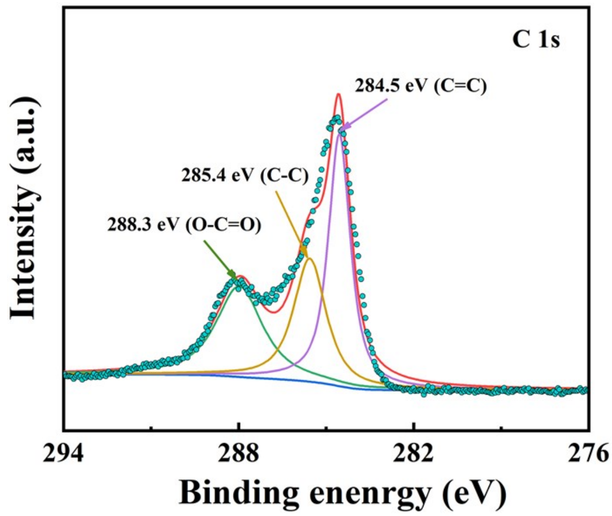

Fig. S2 C 1s spectrum high-resolution XPS spectrum of Ni-nCPs-1.

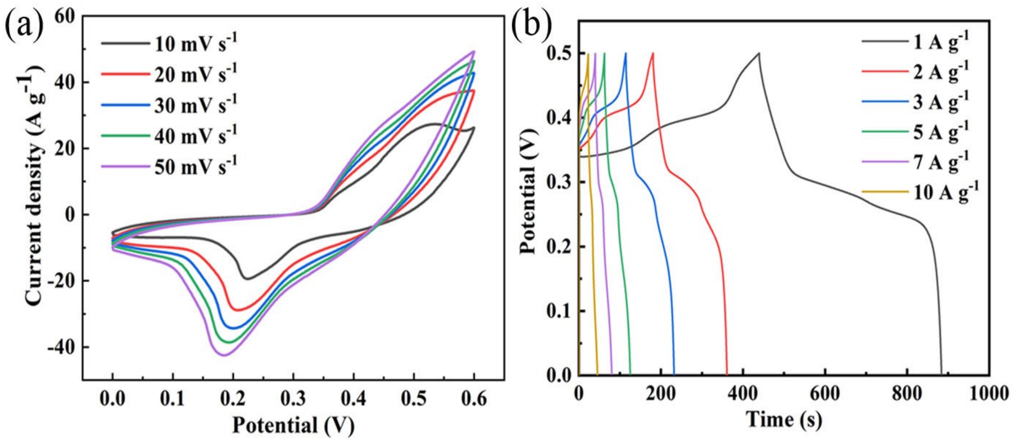

Fig. S3 CV curves (a), and galvanostatic charge/discharge (GCD) curves (b) of Ni-nCPs-2 electrode.

To investigate the electrochemical performance of the Ni-nCPs-2 electrode, cyclic voltammetry (CV) curves with a voltage windows of 0-0.6 V are measured (**Fig. S3a**). Moreover, the galvanostatic charge-discharge (GCD) curves of Ni-nCPs-2 electrode at various current densities (1, 2, 3, 5, 7, 10 A g^{-1}) are tested (**Fig. S3b**), and the corresponding *Cs* values are calculated to be 890.1, 721.3, 715.4, 640.6, 600.1 and 428.3 F g^{-1}, respectively. The plateaus in discharge curves show the increase in capacitance caused by the faradaic redox reaction.

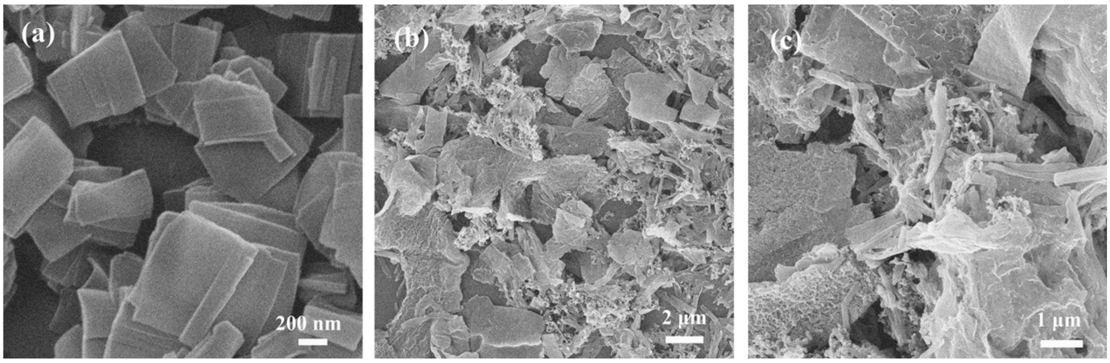

Fig. S4 SEM images pristine (a) and cycled (b, c) sample of Ni-nCPs-1.

Fig. R2a shows the pristine Ni-nCPs-1 has a regular cuboid flaky structure with a relative smooth surface. While, after 3500 cycles, the morphology of Ni-nCPs-1 electrode material becomes irregular, as shown in Fig. R2b, c. Meanwhile, wrinkles and bumps were formed on the surface of the cycled electrode material. The obvious morphology change of the Ni-nCPs-1 electrode material is attributed to constant inflow and outflow of ions and electrons, which plays a negative role in depleting the surface and changing the structural properties of the Ni-nCPs-1 electrode material during cycling process. [1] In turn, the collapse of the morphology inhibits the channels for the ions to diffuse during the electrochemical reaction, resulting in poor capacitance retention. [2]

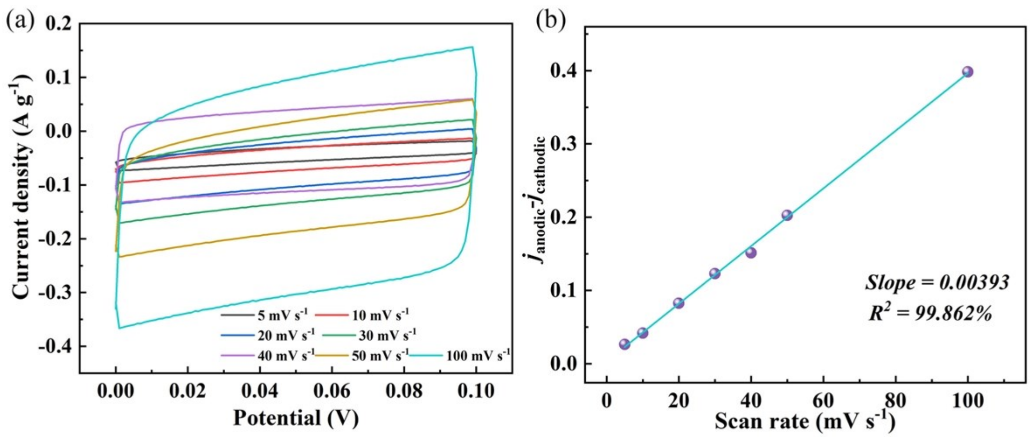

Fig. S5 CV curves of Ni-nCPs-1 using 6 M KOH as electrolyte with the potential ranged from o to 0.1 V (a), the C_{dl} of the obtained Ni-nCPs-1 electrode (b).

As shown in Fig. S3, the CV curves of Ni-nCPs-1 at a narrow potential window (0-0.1 V vs. Hg/HgO) exhibit quasi-rectangular without obvious faradaic peaks at different scan rates. In this range, it is indicated that all capacitance is attributed to the electrical double layer. For Ni-nCPs-1, the difference of anodic current density and cathodic current density at 0.05 V is plotted with the corresponding scan rates. After the linear fit, the specific electrical double layer capacitance (C_{dl}) can be calculated by using the obtained slope in the formula: $C_{dl} = 500 \times Slope$ [3].

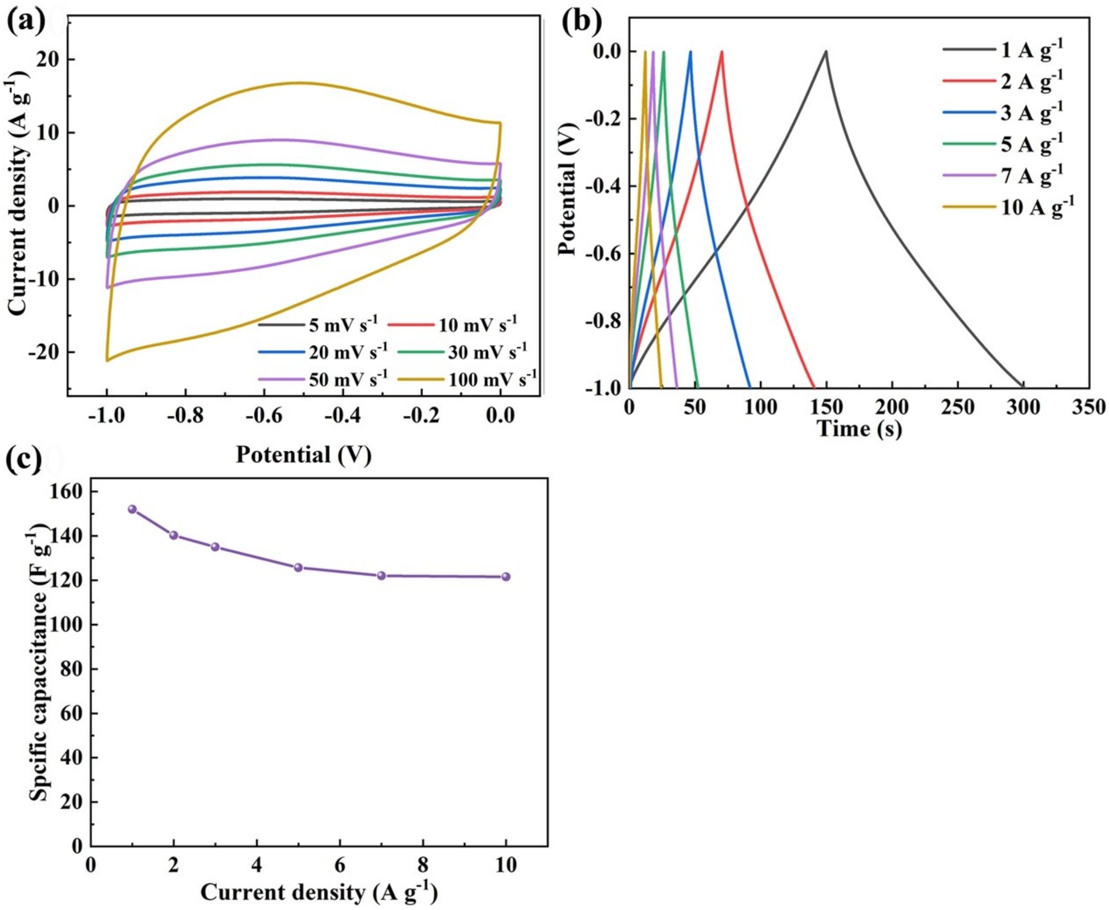

Fig. S6 CV curves of commercial AC at different scan rates (a), GCD curves of commercial AC at different current densities (b), specific capacitance of commercial AC as a function of discharge current density (c).

The AC electrode displays well electrical double-layer capacitance with a quasi-rectangular shape (**Fig. S6a**). The ***Cs*** of AC can up to 152 F g^{-1}, which is calculated from GCD curves from Fig. S4b (**Fig. S6c**).

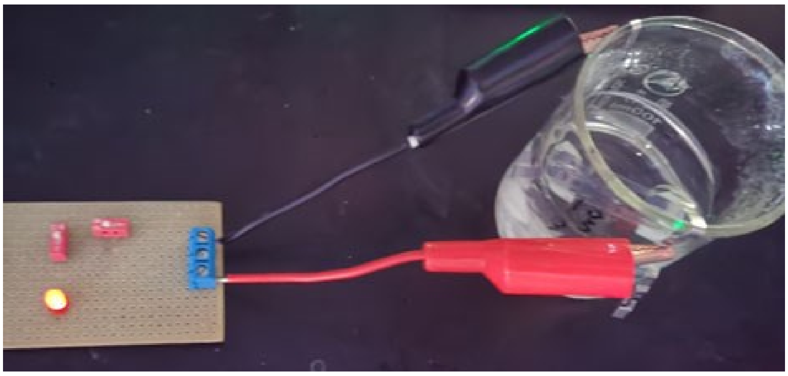

Fig. S7 The photographic image of the ASC device lighting up one LED.

Table. R1 The comparison of the electrochemical property of various Co/Ni-based MOFs

ASC	Curret density (A g^{-1})	$C_{s,\ gcd}$ (F g^{-1})	Energy density (Wh kg^{-1})	Power density (W kg^{-1})	Cycle life		Ref.
					Capacitance retention	Capacitance after cycle (F g^{-1})	
CP1//AC	0.5	23.5	8.36	501.3	90 % over 2000 cycles at 0.5 A·g^{-1}	21.15 F g^{-1} over 2000 cycles at 0.5 A·g^{-1}	[4]
Ni-MOF/rGO-300//AC	1	54.82	17.13	750	81.63% over 4000 cycles at 5 A·g^{-1}	34.08 F g^{-1} over 4000 cycles at 5 A·g^{-1}	[5]
Ni/Co-MOF//AC	1	58.8	20.9	800	85% over 5000 cycles at 3 A·g^{-1}	39.78 F g^{-1} over 5000cycles at 3 A·g^{-1}	[6]
Ni-MOF 1–6 // AC	0.5	87	21	440	70% over 2000 cycles at 5 A·g^{-1}	~ 49 F g^{-1} over 5000 cycles at 5 A·g^{-1}	[7]
Ni-MOF//AC	1	65	16.5	2078	-	-	[8]
Ni-MOF/G//CA	2	~ 87	39.43	342.9	73.6% over 1000 cycles at 2 A·g^{-1}	~ 64 F g^{-1} over 1000 cycles at 2 A·g^{-1}	[9]

Ni-MOF//AC	1	88	31.5	800	50 % over 1000 cycles at 4 $A \cdot g^{-1}$	31 F g^{-1} over 1000 cycles at 4 $A \cdot g^{-1}$	[10]
Ni-nCPs-1//AC	0.5	119.35	47.9	400	46.4 % over 4000 cycles at 3 $A \cdot g^{-1}$	31 F g^{-1} over 4000 cycles at 3 $A \cdot g^{-1}$	This work

It can be seen from the comparison that cyclability of the assembled Ni-nCPs-1//AC ASC does not show a very high value only in terms of the capacitance retention. However, we should notice that the initial capacitance of the as-prepared material is relatively high compared to that of the materials reported in the literature, thus it still maintains an ideal capacitance after 4000 times charging and discharging circulation (31 F g^{-1} over 4000 cycles at 3 $A \cdot g^{-1}$). Therefore, even if the capacitance retention rate of the assembled ASC is slightly unsatisfactory, the actual capacitance after cycling is still considerable. In addition, comprehensively considering the values of energy density and power density, the assembled ASC also shows better performance compared with those Ni-based MOFs reported in the literatures.

Ref:

1. Adhikari, S., Selvaraj, S., Ji, S.H. and Kim, D.H., SMALL, 2020, 16, 2005414.

2. Ghosh, D., Pal, A., Singha, D.K., Ghosh, S., Lebedev, O.I., Seikh,

M.M. and Mahata, P., ACS Applied Nano Materials, 2020, 3, 10105-10114.

3. Wang, Q., Luo, Y., Hou, R., Zaman, S., Qi, K., Liu, H., Park, H.S. and Xia, B.Y., ADV MATER, 2019, 31, 1905744.

4. Zhang, Z., Gao, L., Zhang, J., Niu, X. and Hu, T., J SOLID STATE CHEM, 2020, 292, 121711.

5. Zhong, Y., Cao, X., Ying, L., Cui, L., Barrow, C., Yang, W. and Liu, J., J COLLOID INTERF SCI, 2020, 561, 265-274.

6. Gao, S., Sui, Y., Wei, F., Qi, J., Meng, Q., Ren, Y. and He, Y., J COLLOID INTERF SCI, 2018, 531, 83-90.

7. Du, P., Dong, Y., Liu, C., Wei, W., Liu, D. and Liu, P., J COLLOID INTERF SCI, 2018, 518, 57-68.

8. Kang, L., Sun, S., Kong, L., Lang, J. and Luo, Y., CHINESE CHEM LETT, 2014, 25, 957-961.

9. Azadfalah, M., Sedghi, A. and Hosseini, H., Journal of Materials Science: Materials in Electronics, 2019, 30, 12351-12363.

10. Gao, S., Sui, Y., Wei, F., Qi, J., Meng, Q. and He, Y., J MATER SCI, 2018, 53, 6807-6818.